MucosalImmunology www.nature.com/mi

ARTICLE

A selective window after the food-intake period favors tolerance induction in mesenteric lymph nodes

Bibiana E. Barrios[1], Lisa Maccio-Maretto[1], F. Nicolás Nazar[2] and Silvia G. Correa[1]

Biological rhythms are periodic oscillations that occur in the physiology of the organism and the cells. The rhythms of the immune system are strictly regulated and the circadian alteration seems to have serious consequences. Even so, it is not clear how the immune cells of the intestinal mucosa synchronize with the external environment. Besides, little is known about the way in which biological rhythms affect the critical functions of intestinal immunity, such as oral tolerance. We studied fluctuations in the relevant parameters of intestinal immunity at four different times throughout the day. By using multivariate statistical tools, we found that these oscillations represent at least three different time frames with different conditions for tolerance induction that are altered in Per2ko mice lacking one of the clock genes. Our results allowed us to characterize a window in the final stage of the dark phase that promotes the induction of specific regulatory populations and favors its location in the lamina propria. We show here that, at the end of the intake, the entry of luminal antigens, soluble factors, and leukocyte populations converge in the mesenteric lymph nodes (MLN) and display the greatest potential of the tolerogenic machinery.

Mucosal Immunology _####################_; https://doi.org/10.1038/s41385-018-0095-3

INTRODUCTION

Biological rhythms are periodic oscillations that occur in the physiology of the organism and the cells[1]. Circadian rhythms have a periodicity of approximately 24 h and they are adjusted to different geophysical conditions[2]. In mammals, the circadian system is organized in a hierarchical manner with a specialized center in the hypothalamus, the suprachiasmatic nucleus (SCN), which synchronizes the organism to the external photoperiod[1,3]. Although circadian oscillators described in most peripheral tissues may be coordinated by the SCN, they can also be entrained by external cues, known as zeitgebers (i.e., time givers)[4]. Light is considered the key entrainment factor for the SCN, whereas peripheral cells and tissues are synchronized with the environment by a complex network involving neuronal signaling, hormone secretion, and metabolic clues derived from the rhythmic feeding behavior[5]. Circadian rhythms are driven by autonomous biological clocks that consist of a network of transcription factors in each cell, including period (Per), cryptochrome (Cry), Bmal (Arntl), and Clock, with nuclear receptors of the ROR and REV-ERB families stabilizing the core oscillator[6]. The circadian clock adjusts physiological processes to different cues by coordinating transcriptome oscillations, which allow the organism to adapt to and anticipate temporal changes in the environment[2]. Most circadian rhythm-related research has focused on the central clock and less attention has been directed towards peripheral tissues.

Under normal circumstances, the immune system is tightly regulated by intrinsic clocks together with inputs from the central pacemaker of the SCN[7]. The disruption of circadian rhythms seems to have severe consequences, as circadian rhythms promote inflammatory processes[8]. In the intestine, circadian disruption results in increased intestinal Th17 cells[9], higher rates of infection[10], and robust proinflammatory responses to lipopolysaccharide[11]. It has recently been shown that intestinal microbiota undergoes diurnal fluctuations in community populations and in bacterial functions such as the metabolism, which can be affected by the host's feeding time and diet composition[4]. On the other hand, microbial products and feeding rhythms are powerful cues for the synchronization of peripheral tissues[12] and, when the circadian feeding rhythm is disrupted, it induces a variety of diet-dependent metabolic, immune, and gastrointestinal alterations[13]. However, it still remains unclear how mucosal immune cells are synchronized in vivo to the external environment. Besides, very few studies have been conducted about the effects of rhythms on the intestinal mucosa, and little is known about the way biological rhythms affect its core functions, such as oral tolerance.

Herein, we studied fluctuations in relevant parameters of intestinal immunity at four different times throughout the day. By using multivariate statistics tools, we found that these oscillations account for at least three distinct time windows with different conditions for tolerance induction. These windows are altered in Per2ko mice, which suggests that they depend on the clock machinery. Our results indicate that entry of luminal antigens into the mesenteric lymph nodes (MLNs) by the end of the dark phase promotes the induction of specific regulatory populations and favors their localization in the lamina propria.

RESULTS

Taking into account the transcriptional basis of circadian rhythms, we first evaluated *Per2* and *Bmal1* transcripts in MLNs of WT mice

[1]Centro de Investigaciones en Bioquímica Clínica e Inmunología (CIBICI, CONICET-UNC), Departamento de Bioquímica Clínica-Facultad de Ciencias Químicas, Universidad Nacional de Córdoba, Córdoba CP 5000, Argentina and [2]Instituto de Investigaciones Biológicas y Tecnológicas (IIByT, CONICET-UNC) e Instituto de Ciencia y Tecnología de los Alimentos, Facultad de Ciencias Exactas, Físicas y Naturales, Universidad Nacional de Córdoba, Córdoba CP 5000, Argentina
Correspondence: Silvia G. Correa (scorrea@fcq.unc.edu.ar)

Received: 12 July 2018 Revised: 3 September 2018 Accepted: 16 September 2018
Published online: 16 October 2018

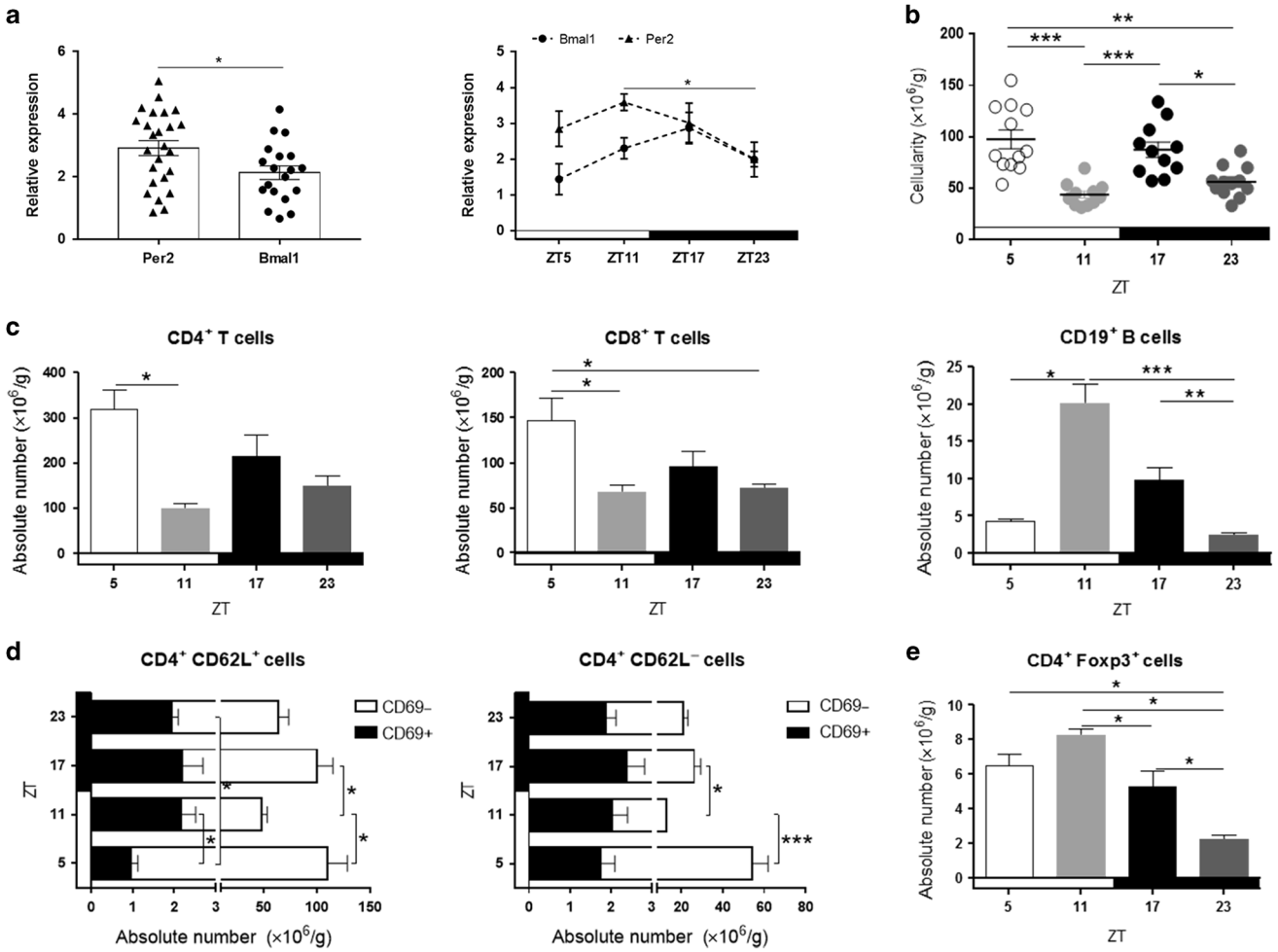

Fig. 1 Clock gene transcripts and cell subsets in MLNs over a 24-h period. MLNs from WT mice under standard light–dark conditions were removed at ZT5, 11, 17, and 23. **a** mRNA was obtained as described in "Materials and methods" and transcription of Bmal1 and Per2 clock genes was performed by real-time PCR. Data were relativized with GADPH gene expression and represented as total expression (left) or at different ZT (right). **b** Absolute number of leukocytes per gram of tissue. **c** Absolute number of CD4+, CD8+, and CD19+ lymphocytes per gram of tissue assessed by flow cytometry. **d** Expression of the CD69 marker in CD4+CD62L+ or CD4+CD62L− lymphocytes per gram of tissue assessed by flow cytometry. **e** Absolute number of CD4+Foxp3+ cells per gram of tissue over a 24-h period, evaluated in Foxp3-GFP animals kept under standard light–dark conditions by flow cytometry. Data are individual and mean values ± SEM of $n = 19$–25 (panel **a**) or $n = 7$–12/ZT. *$p < 0.05$; **$p < 0.01$; ***$p < 0.001$

at ZT5, 11, 17, and 23. All mice were fed ad libitum and housed under strict 24-h dark–light conditions, with lights on for 12 h starting at 7 a.m. (ZT0). As can be seen, these clock genes were expressed in the lymphoid tissue at the different times of evaluation, showing higher levels of Per2 transcripts (Fig. 1a, left) and a significant fluctuation for Per2 over a 24-h period, with highest expression at ZT11, lowest at ZT23, and intermediate at ZT5 and 17 (Fig. 1a, right). In this mucosal inductive site, cellularity showed a marked oscillation, with peaks at around ZT5 and 17 (Fig. 1b). This pattern was mostly determined by CD4+ and CD8+ T lymphocytes, which rose in the middle of the diurnal period (Fig. 1c). Conversely, B cells and CD4+Foxp3+ cells had a different pattern, with the highest counts at the end of the diurnal phase (ZT11, i.e., 1 h before lights were off) (Fig. 1c, e). Oscillations were consistently observed for naive CD4+ CD69− T cells, either CD62L + or CD62L−, with count peaks at ZT5 and 17 (Fig. 1d).

To study the signals driving these oscillations, we evaluated CCL-21 levels in MLN homogenates. Consistently, oscillations in this chemoattractant (Fig. 2) paralleled changes in cellularity detected in MLNs, with significant increments during the diurnal phase ($p < 0.05$). We also determined the cytokine milieu in MLNs at the different ZT in cultures of stimulated mononuclear cells. After 48 h, IL-10 predominated at ZT5, with a similar trend for IL-4 and IL-22. On the other hand, the inflammatory profile showed an opposite pattern, with significant peaks at ZT11 and 23 for IL-23 (Fig. 3).

We hypothesized that the oscillatory patterns found in cell subsets and soluble mediators at the inductive sites might have functional consequences in intestinal effector immune responses. To address this possibility, we performed a principal component analysis (PCA) taking into account 17 parameters (see Supp. Table 1) and including time as a classification criterion. The PCA biplot of MLN parameters (Fig. 4a) shows a distribution in four ZT clusters in an *n*-dimensional space. The 73.8% variability was represented by the first two principal components (PC) in the biplot: PC1 explains 50.7% and PC2 explains 23.1%. Subsequently, according to the eigenvector values and the biological relevance for mucosal responses, we selected four variables from the PCA (Supp. Table 1) to perform a linear discriminant analysis (LDA). As can be seen, the LDA defined three different temporal categories: ZT5, ZT17, and ZT11–ZT23, which showed a partial overlapping, suggesting that these could be transition times (Fig. 4b). The multivariate ANOVA test (MANOVA) of these four subgroups confirmed that ZT5 and ZT17 describe potentially different

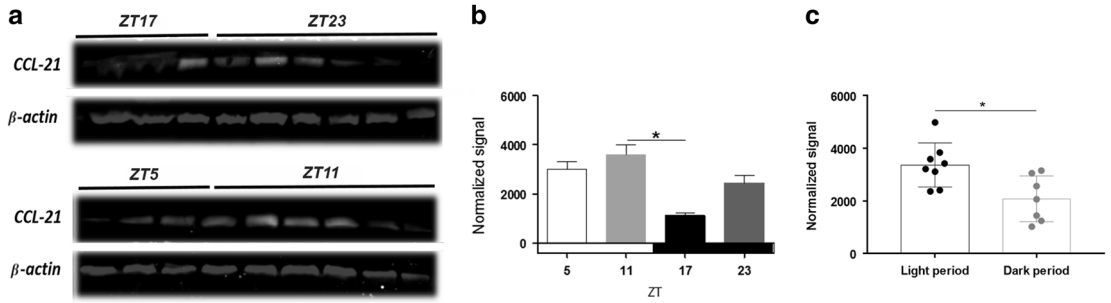

Fig. 2 CCL-21 expression in MLNs over a 24-h period. Levels of CCL-21 were analyzed in MLN homogenates from WT mice at ZT5, 11, 17, and 23. Representative Western blot (**a**). Data were normalized with β-actin expression and represented at different ZT in light (**b**) or dark periods (**c**). Means ± SEM of $n = 3–5$/ZT. *$p < 0.05$

immune settings ($p < 0.0001$), whereas ZT11 and ZT23 represent stages with a similar functionality (Supp. Table 2). Interestingly, ZT11 and ZT23, that showed considerable overlapping in terms of functionality, exhibited significant differences in Per2 transcript expression (Fig. 1b). The PCA, LDA, and MANOVA confirmed that MLNs present circadian differences in functional capacities. In conclusion, the intestinal mucosal immune system in the steady state could be under the influence of a biological clock. The observed rhythms could condition immune responses to different stimuli throughout the day.

If the functionality of the mucosa is effectively regulated by the biological clock, the deficiency in some components of this machinery may alter the parameters that oscillate in WT mice. To evaluate this possibility, we performed both PCA and LDA (not shown) analyses in WT and Per2ko mice. In the absence of the Per2 gene, the variability in essential elements of the immune function was reduced over time, possibly contracting plasticity to the mucosal response. As can be seen, Per2ko mice presented a less variable distribution, with a lower discrimination between the four ZT studied (Fig. 5). By contrast, WT mice showed marked fluctuations throughout the day, as described above.

Tolerance is a central response in intestinal mucosa and it depends both on the continuous sampling of antigens and the activity of professional antigen-presenting cells (APC) that migrate from the lamina propria to MLNs. We thus evaluated the amount of cells with a high MHC-II expression in MLNs at different ZT (Fig. 6a, left). The absolute number of MHC-II+ cells fluctuated throughout the day, with a significant increase towards the end of the diurnal phase (ZT11). Additionally, we analyzed intestinal dendritic cells (iDC) in transit through the afferent lymphatic vessels (ALV) as previously described[14]. The frequency of CD11c+ MHC-II+ iDC in ALV was significantly higher during the night ($p < 0.05$) at feeding time (Fig. 6a, middle). Both during the dark (Fig. 6a, right) and the diurnal (not shown) phases, the frequency of CD11c+ CD11b^{low} was higher. Considering that cells involved in tolerance induction express the CD103 marker and carry vacuoles containing Muc-2 protein and bacteria[15], we evaluated the presence of Muc-2 by Western blot in cells isolated from MLNs and ALV. Figure 6b (left) shows a representative experiment where Muc-2 is present both in MLNs and in migrating cells at the different times studied. Interestingly, levels of Muc-2 in ALV cells were significantly higher at ZT5 (Fig. 6b, right). The APC transporting Muc-2 isolated from ALV at ZT5 were mostly CD11c + CD103+ iDC; still, we found F4/80+ MHC-II+ Muc-2+ macrophage-like cells also positive for fractalkine receptor CX3CR1 (Fig. 6c).

The two potentially different immune settings defined based on multivariate analyses (ZT5 and ZT17) and the phenotype of iDC Muc2+ isolated at ZT5, suggested that this particular ZT could be a critical window for the tolerance induction. Providing that the most relevant functional competence of iDC CD103+ is to generate regulatory cells, we evaluated in vitro the ability of APC isolated at different ZT to induce Foxp3 expression in CD4+ Foxp3− cells sorted from Foxp3-GFP mice. As can be seen, APC obtained at ZT5 showed the highest ability to induce Foxp3 expression after co-culture (Fig. 7a), reinforcing the concept that ZT5 could be the critical period for tolerogenic activity. Considering the following evidence: (a) Muc2+ APC were more abundant at ZT5 (Fig. 6); (b) APC isolated at ZT5 showed the highest tolerogenic potential in vitro (Fig. 7a); (c) LDA and MANOVA demonstrated that ZT5 and 17 represent potentially different immune settings (Fig. 4b and Supp. Table 2); and, (d) early activation of T lymphocytes—which involves the interaction with APC—already occurs 6 h after antigen feeding[16], an in-vivo experiment was designed to test the possibility that ZT5 could be the critical window for tolerance induction. CD45.2+ CD4+ OT-II OVA-specific cells were transferred to WT CD45.1+ mice. Then, the recipients were treated with 1.5% OVA, starting at ZT11 or ZT23 as described in "Materials and methods". After 6 days, the expression of Foxp3 (regulatory cells) and Tbet (Th1 cells) was evaluated in CD45.2+ cells in MLNs, the spleen, and the lamina propria (Fig. 7b). Oral administration of the specific antigen at the two evaluated ZT reduced the number of Foxp3+ cells in MLNs ($p = 0.06$). Notably, when antigen administration started at ZT23, the amount of Foxp3+ OVA-specific cells increased significantly in the lamina propria. Interestingly, if antigen administration started at ZT11, Foxp3+-specific cells were detected mainly in the spleen. No differences were found in the number of specific Tbet+ cells for any tissue studied, but the Foxp3/Tbet ratio was significantly higher in the lamina propria of tolerized mice starting at ZT23. These findings demonstrate that, at the end of the feeding period (~ZT5), MLNs present conditions prone to tolerance induction.

DISCUSSION

Studying biological rhythms has acquired fundamental importance to understand physiological events as well as imbalances that lead to pathologies. In the intestine, microbial products are powerful cues for the synchronization of mucosal tissues[12] and circadian disruption results in increased intestinal Th17 cells[9] as well as in diet-dependent metabolic, immune, and gastrointestinal alterations[13]. However, very few studies address the way biological rhythms affect critical functions, such as oral tolerance. In this work, we have characterized the influence of biological rhythms in the intestinal mucosal immune function throughout the day. Specifically, we have described some mechanisms that govern the temporal location of different leukocyte populations in inductive sites of the intestinal mucosa, as well as their impact on key phenomena of homeostasis, such as tolerance to antigens from the diet.

Our results show that Per2 levels were higher throughout the day, with significant fluctuations in MLNs, while Bmal1 expression exhibited no changes. Similarly, by using a specific algorithm to determine rhythms, other authors showed that Bmal1 undergoes

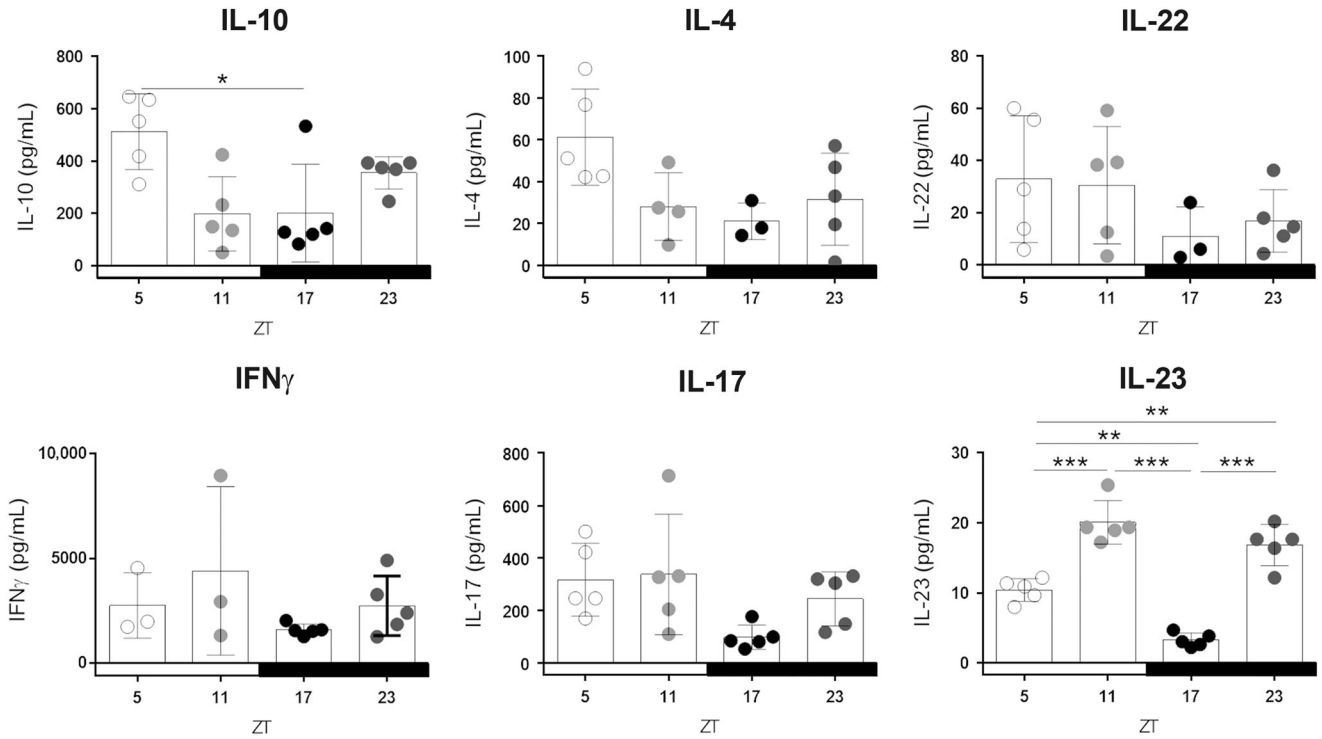

Fig. 3 Production of cytokines by mononuclear cells from MLNs over a 24-h period. Mononuclear cells (1×10^6 cells) were stimulated with anti-CD3/anti-CD28 for 48 h and different cytokines were measured in supernatants by ELISA. Means ± SEM of $n = 3$–5/ZT. *$p < 0.05$; **$p < 0.01$; ***$p < 0.001$

no significant circadian oscillations in B lymphocytes, macrophages, or DCs isolated from the spleen[17,18]. Circadian gene expression is remarkably tissue-specific and, in many cases, it involves rate-limiting steps that are distinct for the functions of a particular organ[19]. Considering that MLNs are a heterogeneous immunological tissue composed of different cell types—some of which fluctuate in absolute or relative numbers—differences in transcript levels of the genes described in this work could be mutually compensating, thus adding complexity to the analysis, as previously suggested[20]. The presence of both genes in MLNs corroborates what other authors have found in tissues associated with the intestine. It also suggests that the functioning of a biological clock may regulate key processes not only of the intestinal physiology but also of the immune function linked to the specific activity of this tissue[21].

We found oscillations in the cellularity in this inductive site with significant increases during both the light (ZT5) and the dark (ZT17) phases. These results agree with the rhythms described in the cellularity of several types of lymph nodes, indicating that oscillations constitute a relevant phenomenon of the lymphoid compartment[22]. Cellularity dynamics in secondary lymphoid tissues seems to be a broad and robust phenomenon, not restricted to particular sites of the organism that depends on both environmental factors and the specific expression of molecules on the cell surface[22,23]. The absolute number of CD4+CD62L+ cells increased mainly at ZT5 and ZT11, whereas CD8+ lymphocytes remained constant throughout the day. These fluctuations could be related to changes in CCL-21 levels, as well as to the differential expression of CD69. Indeed, entry into and exit from lymph nodes are regulated by factors with antagonistic function such as CCL-21 and sphingosine-1-phosphate (S1P), the oscillation in their respective receptors—CCR7 and S1PR1, and molecules such as the early activation marker CD69[22]—which prevents cell egress by physical association with S1PR1[24]. In our experimental system, despite the increase in cell count, CD69 expression was lower in CD4+ and CD8+ T lymphocytes at ZT5. This reduction could account for the decrease observed later at ZT11, since more cells could be ready to leave the MLNs. In turn, reduced levels of CCL-21 at ZT17 could explain the lower cellularity observed 6 h later (i.e., ZT23). Regarding the possible significance of these fluctuations, CD4+ T cells responding to the endogenous peptide–MHC complex transiently increase CD69, and their exit is delayed compared to other T cells, which has a basal influence on lymphocyte recirculation[25]. That is, transient or weak TCR stimulation that is sufficient to increase CD69 will retain T cells within nodes to favor encounters with iDC and thus produce full activation or tolerance induction[26], a continual situation at the intestinal mucosa. At the end of the food intake (ZT5), higher IL-10 and lower IL-23 could be traits of a period with extremely favorable conditions for the induction of tolerance towards diet-derived antigens. In fact, MLNs are the crucial sites involved in oral tolerance induction[27] and IL-10, a powerful regulatory cytokine, is directly involved in intestinal inflammation control[28,29]. Moreover, IL-10 reduces production of IL-23 by inhibiting the expression of p19 subunit[30].

The absolute number of MHC-II+APC increased towards the beginning of the dark phase (ZT11), prior to the massive entry of antigens that would take place during the food-intake period. Changes in different populations of APC oscillating throughout the day in MLNs show that not only the entry of lymphocytes is subject to biological rhythms, but also the populations that transport dietary and microbial antigens from the lumen[31,32]. It has been shown that local oscillations in the expression of pro-migratory factors (i.e., chemokines or receptors) affect homing probability at particular stages of the day[33,34], and that certain nutrients and the feeding time synchronize peripheral clocks[21]. Accordingly, the loss of these patterns (at least partially) in mice with a deficient clock gene suggests that this molecular machinery coordinates the leukocyte traffic towards inductive sites at different levels[33]. Our results show that APC flux was not continuous during the day, but described fluctuating patterns orchestrated by signals such as CCL-21 or the intrinsic oscillatory

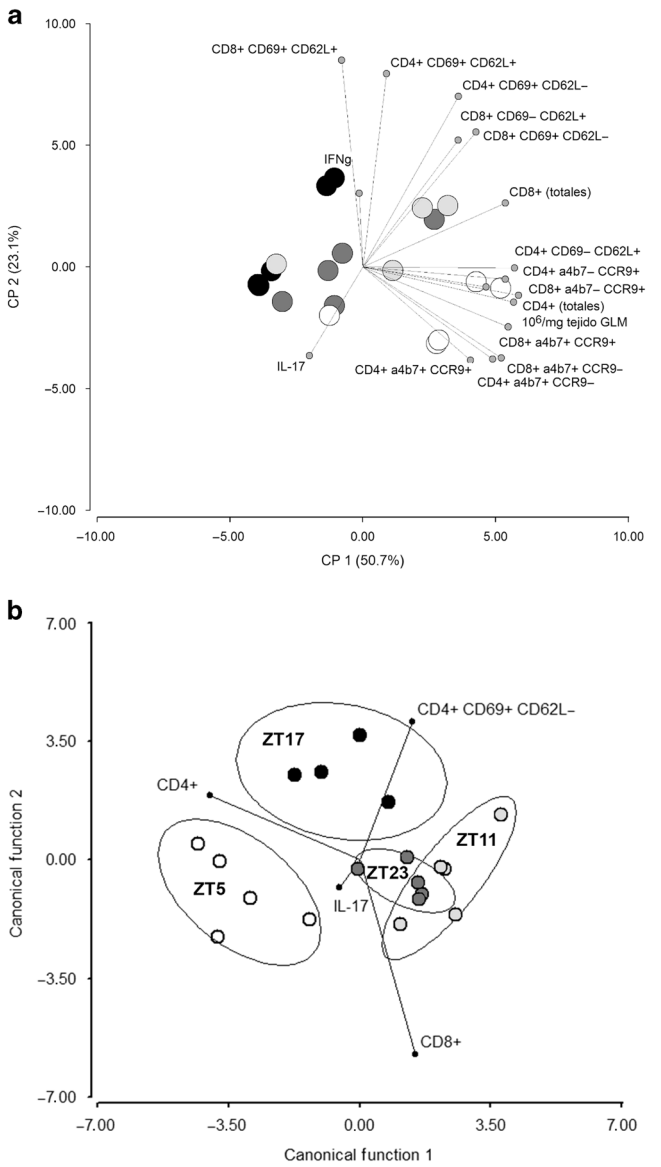

Fig. 4 Multivariate analysis assessed over a 24-h period. **a** Principal component analysis (PCA); biplot of PC1 and PC2 considering 17 parameters at ZT5, 11, 17, and 23 in MLNs from WT mice. **b** Linear discriminant analysis (LDA) taking into account absolute numbers of CD4+ and CD8+ T cells, CD4+CD69+CD62L− cells, and the production of IL-17 cytokine. Ellipses include mice with similar values for each one of the four variables and classified according to ZT time points

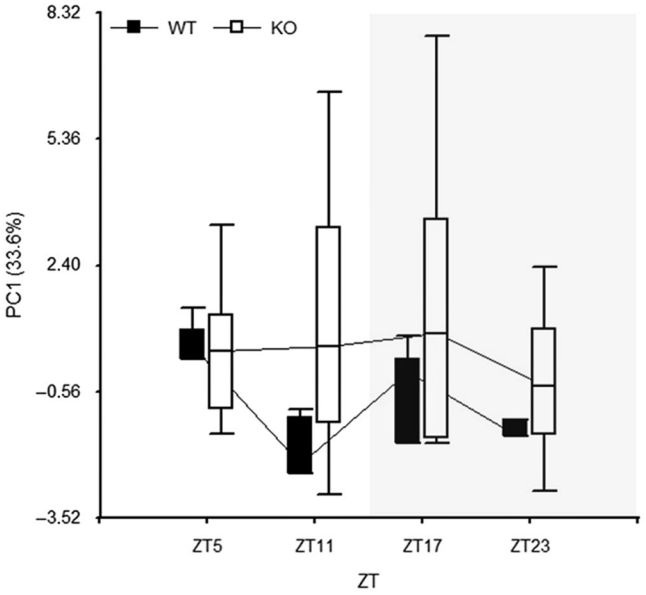

Fig. 5 Representation of principal component in WT and Per2ko mice. PCA considering 17 parameters was performed in WT and Per2ko mice as described in Fig. 4. PC1 at different ZT for both strains is depicted

activity of microbiota[35], which can program the host transcriptomic oscillations[12]. Remarkably, APC isolated from ALV at ZT5 transported higher levels of Muc-2, a signal that improves the tolerogenic functions of iDC, including the production of TGFβ, IL-10, or retinoic acid[36]. It must be highlighted that Per1/2-deficient mice have a lower number of goblet cells along with a low Muc2 gene expression and that both the diminished number and the loss of function of goblet cells have been linked to intestinal inflammation[37]. While this report emphasizes the relevance of Per1/2 genes in the shaping and integrity of the epithelial barrier, our data demonstrate the importance of circadian variation in the activity at the inductive sites. Interestingly, Muc-2 was found in both migratory CD103+ iDC and in F4/80+ CX3CR1+ macrophage cells of afferent vessels. In agreement with this, iDC pick up Muc-2 by interacting with goblet cells or through vesicles containing Muc-2 released by epithelial cells[15]. On the other hand, CX3CR1^{hi} cells present in the afferent lymph of non-manipulated mice are a novel pathway for the access of luminal antigens for immune priming[38]. In conclusion, ZT5 could be the temporal window that may favor tolerogenic responses to oral antigens.

Similarly to innate immunity under circadian control, adaptive immune responses also appear to be regulated in a circadian fashion[20,32,33,39]. After adoptive transfer of specific CD4+ OT-II+ OVA cells, the differences found in the induction of Foxp3+ T cells confirmed that the diurnal period favors tolerogenic responses to antigens coming from the food-intake period. The immune response to specific antigenic challenges throughout the day seems to rely on the tuning to the oscillations of the different factors involved[22,39–42]. In fact, in murine models of allergy to dietary antigens using OVA, Tanabe et al. demonstrated that oral administration of the antigen during the light period induced greater severity in allergy symptoms compared to administration during the dark period[42]. This severity was accompanied by a higher production of cytokines from the Th2 profile (IL-13 and IL-5), increased diarrhea and weight loss. Interestingly, after OVA administration, Foxp3+ cells were mainly located in the lamina propria only when antigen administration started at ZT23. However, when the antigen was administered from ZT11, specific Foxp3+ cells were concentrated in the spleen. According to our data, oral tolerance, in addition to its systemic effects, acts locally in the intestine, thereby preventing the chronic inflammatory phenomena that result from excessive reactivity against dietary antigens[43]. Changes in the number of CD4+ cells in lymph nodes during the first contact with the antigen have an important effect in the severity of different inflammatory diseases or allergy to food antigens[22,42]. Moreover, in our system, the increment in the absolute number of regulatory CD4 + Foxp3+ T cells during the light phase in MLNs corresponded with the lower activation status of CD4+ lymphocytes (Fig. 1d, e). This emphasizes the concept that the exact moment of antigen administration and the antigen's subsequent encounter with specific cells are decisive for inducing Foxp3 regulatory cells capable of conditioning tolerance at the peripheral level. In this

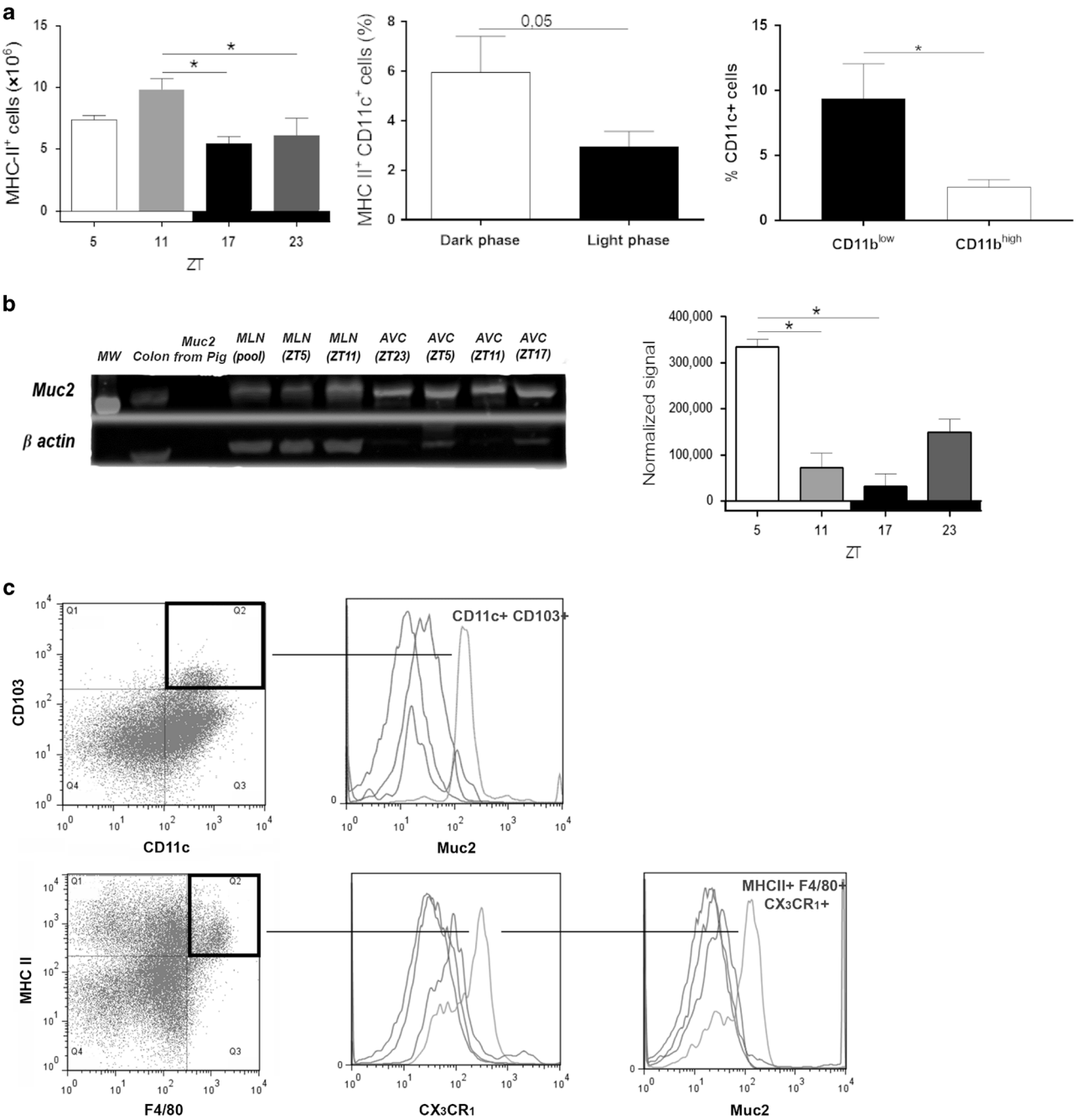

Fig. 6 Evaluation of APC in afferent lymphatic vessels (ALV) and MLNs during a 24-h period. **a** Absolute number of MHC-II+ cells per gram of tissue was evaluated in MLNs of WT mice at ZT 5, 11, 17, and 23 (left). Frequency of MHC-II+ CD11c+iDC present in ALV during light or dark period (middle) and MHC-II+ CD11c+ CD11b^{high} and MHCII+ CD11c+ CD11b^{low} during dark phase (right). **b** Representative determination of Muc-2 glycoprotein in ALV collected cells and MLN homogenates by Western blot at ZT5, 11, 17, and 23. Colon homogenate and mucine type II from pig were used as controls. **c** Phenotype characterization of Muc-2+ APC present in ALV at ZT5 evaluated by intracellular flow cytometry. Representative dot plots of Muc-2 determination in CD11c+CD103+ iDC and MHC-II+ F4/80+CX3CR1+ macrophages. Data are means ± SEM; $n = 3$–5/ZT. *$p < 0.05$; ***$p < 0.001$

regard, a model has been proposed to generate regulatory cells in stages. The first one involves the activation of specific antigen naive cells in the MLNs to generate a founder nucleus that will colonize the intestinal lamina propria (it is the latent tolerance). The second phase involves the homing and "irreversible" installation of tolerogenic effector cells in tissues exposed to the antigen, where cell expansion takes place due to the effects of signals from resident cells[43]. There is considerable consensus that Foxp3+ regulatory T cells in the intestine are located primarily in the lamina propria[44,45].

In general, it has been proposed that the immune system oscillates between two phases throughout the day: one represented by an intense state of alert when the animal prepares for the transition to activity and the risk of infection or injury is greater, and a second state when the animal rests and the risk of infection or injury is reduced. This state may provide an opportunity to reduce inflammation and repair tissues[8]. Our work moves toward this conceptualization, demonstrating the significant influence of the circadian clock machinery on the functioning of the immune system in the intestine and its physiological

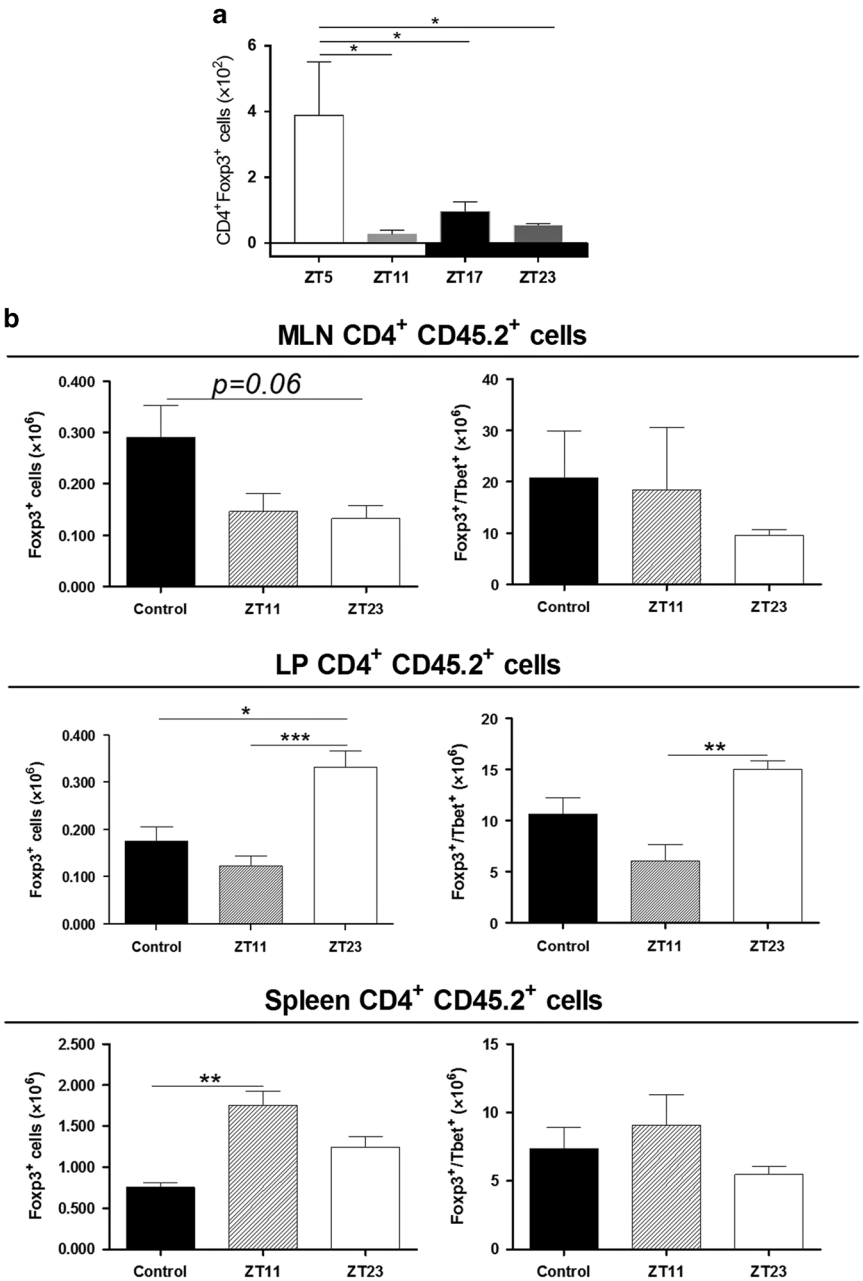

Fig. 7 In vitro and in vivo assessment of APC tolerogenic capacity at different ZT. **a** ALV cells were isolated at ZT5, 11, 17, and 23 and cultured for 96 h at a 1:1 ratio with CD4+ Foxp3-GFP− lymphocytes purified from MLNs by sorting as described in "Materials and methods". After culture, CD4+ Foxp3-GFP+ cells were evaluated by flow cytometry. Data were expressed as absolute numbers. **b** CD45.1+ mice transferred with CD4+ CD45.2+OT-II+ cells and after 24 h, recipients received 1.5% OVA in drinking water for 6 days beginning at ZT11 or 23 or no treatment (control group). Frequency of CD4+CD45.2+OT-II+Foxp3+ or Tbet+ cells in MLNs, the lamina propria, and the spleen. Data were expressed as frequency of Foxp3 or Foxp3/Tbet ratio. Means ± SEM of $n = 4$/ZT. *$p < 0.05$; **$p < 0.01$; ***$p < 0.001$

connotations. Here, findings demonstrate that throughout a day at least three functionally distinct temporal categories can be found in the MLNs (Fig. 4). Moreover, we describe a possible linking path between opposite stages (ZT5 and ZT17) by intermediate transitional categories (ZT11 and ZT23). Remarkably, those categories that were functionally similar showed different clock gene transcriptional activity, possibly anticipating the functional differences observed 6 h later, i.e., at ZT5 and ZT17. In summary, our results allowed us to characterize a temporal window at the final stage of the animals' greatest activity (ZT5) where different factors and leukocyte populations converge in the MLNs to display the machinery of tolerance to its greatest potential.

MATERIALS AND METHODS

Mice

The wild-type (WT) and knockout mice used in this study have a C57BL/6 background. The C57BL/6 (WT CD45.1+/+ or CD45.2+/+), Per2−/− (B6.Cg-Per2<tmBrd>Tyr <o-), Foxp3-GFP, and OT-II+/− T cell receptor transgenic mice (specific for the K^b-restricted ovalbumin 257–264 epitope ($OVA_{257–264}$)) were purchased from Jackson Laboratories. For all experiments, the mice were maintained in specific pathogen-free conditions and housed in collective cages at 22 ± 2 °C under a 12-h light/dark cycle (lights on at 7:00 a.m.; ZT0) with free access to laboratory chow and drinking water. Animals of 6–8 weeks of age were analyzed at ZT5,

11, 17, and 23. All animal experiments were approved by and conducted in accordance with the guidelines of the Committee for Animal Care and Use of Facultad de Ciencias Químicas, Universidad Nacional de Córdoba (Approval No. RD 1421/2012), in strict accordance with the recommendations of the Guide to the Care and Use of Experimental Animals published by the Canadian Council on Animal Care (OLAW Assurance No. A5802-01). Our animal facility obtained NIH animal welfare assurance (Assurance No. A5802-01, Office of Laboratory Animal Welfare, NIH, Bethesda, MD, USA).

Reagents and antibodies

The following fluorophore-conjugated antibodies were purchased from BD PharMingen (San Diego, CA): anti-CD3 (17A2), anti-CD28 (37.51), anti-CD4 (GK 1.5), anti-CD8 (53–6.7), anti-CD19 (1D3), anti CD62L (MEL-14), anti-CD69 (H1.2F3), anti-CD11c (HL3), anti-CD11b (M1/70), anti-CD103 (M290), anti-F4/80 (BM8), anti-MHC-II (25-9-17), anti-CX3CR1 (cat. FAB5825A), and anti-CD45.2. Corresponding isotype-matched monoclonal antibodies were used as controls in flow cytometry experiments. For intracellular staining (Foxp3 and T-bet transcription factors), the cells were permeabilized with the fixation/permeabilization kit (eBioscience) and stained with the antibodies according to the manufacturer's instructions.

The flow cytometry was performed with a BD FACS CantoII (BD Biosciences) and the data were analyzed using FlowJo software (Treestar). Sorting experiments were performed with an FACS Aria Fusion (BD Biosciences).

Real-time PCR

The evaluation of mRNAs for Bmal1 clock genes (ID: Mm00500226_m1), Per2 (ID: Mm00478113_m1), and GADPH (ID: Mm99999915_g1) was performed using TaqManGene Expression Assay from Thermo Fisher Scientific. Total RNA was extracted with TRIzol® (Life Technologies, Gibco) and quantified. Reverse transcription was performed, as previously described, in a final volume of 20 µL[46].

Real-time PCR was performed on the Step One Plus Detection System (Real-Time PCR System—Thermo Fisher Scientific). Each reaction mixture had 1 µL of cDNA with 0.3 µL of the corresponding sense and anti-sense primers, 6 µL of 2× TaqMan® Master Mix (Applied Biosystem, Life Technologies, Brazil), and DEPC water to complete a total volume of 12 µL per sample. Each run was performed with a 10-min cycle at 95 °C for the activation of the polymerase enzyme, followed by 40 cycles of 95 °C for 10 s and 60 °C for 1 min. Expression of the target genes was relativized with GADPH and calculated using the ΔΔCT method.

Western blot

CCL-21 was determined in MLN homogenates as described[46]. Bands were analyzed with the Image Studio Lite Software (Lincoln, NE, USA), normalized with β-actin and expressed as relative units.

Cell isolation

MLNs draining jejunum and proximal and distal ileum[47] were removed from the abdominal cavity, cleaned from fat tissue, and processed by mechanical disruption through a mesh. The colonic cells in the lamina propria were isolated as previously described, with slight modifications[48,49]. Briefly, the extraintestinal fat tissue and blood vessels were carefully removed and the intestines were flushed with cold PBS, opened longitudinally, and cut into ~0.5 cm pieces. Epithelial cells and mucus were removed by 15-min incubation in dithiothreitol (DTT) (1 mM) (Sigma-Aldrich, Saint Louis, MO, USA) at 37 °C and shaken at 200 rpm. The tissue was then incubated twice in EDTA (0.5 mM) solution for 30 min each at 37 °C and shaken at 200 rpm. The intestinal pieces were finally digested three times in Collagenase IV solution (5 µg/ml) (Roche) each for 45 min at 37 °C in a shaker. The digested cell suspension was washed with PBS and passed through 40-µm cell strainers. The isolated lamina propria cells were resuspended in complete RPMI medium.

The spleen was processed by mechanical disruption through a mesh. The cell suspension was centrifugated and the pellet was resuspended in 1 ml of lysing buffer (Sigma) for 5 min to lyse erythrocytes. After PBS addition, the cell suspension was centrifuged at 1500 rpm for 5 min. The supernatant was discarded and the pellet was resuspended in 2 ml of media culture until use.

The cells were isolated from ALV as previously described[14]. Briefly, the small intestine, together with the mesentery and the appendix, were extracted from the peritoneal cavity at ZT5, 11, 17, and 23. The intestine was arranged in a fan shape on a flat surface; the adjoining sections of the mesentery containing ALV were removed and incubated in 10% fetal calf serum-RPMI to allow cells to migrate without further manipulation. After 3 h, ALV were removed carefully, the cells were recovered by gentle centrifugation and then stained for flow cytometry.

Cell culture and cytokine measurement

Single-cell suspensions (1×10^6 cells/ml) from MLNs obtained at ZT5, 11, 17, and 23 were cultured in RPMI-1640 medium supplemented with 10% fetal calf serum and antibiotics. The cells were stimulated with 2 µg/ml of anti-CD3 and 1 µg/ml of anti-CD28 antibodies. The supernatants were harvested 48 h later and assayed for IL-4, IL-10, and IFNγ (BD Pharmingen, San Jose, CA) or IL-17, IL-22, and IL-23 (R&D System) using ELISA kits, as specified by the manufacturers[48,49].

In vitro Foxp3 induction

Cells from the ALVs were isolated at ZT5, 11, 17, and 23, as previously described[14]; CD4+ Foxp3-GFP− lymphocytes were purified from MLNs by sorting on a FACS Aria (BD Biosciences) at 8 a.m. (for cultures with ALV obtained at ZT 23 and 5) or 11 a.m. (for cultures with ALV obtained at ZT 11 and 17). APC from different ZT and CD4+ Foxp3-GFP− lymphocytes were cultured for 96 h at a 1:1 ratio, and then evaluated by flow cytometry.

In vivo T cell conversion assays

The CD4+ T cells were purified from the spleen and MLNs of OT-II +/− CD45.2 mice by sorting on a FACS Aria (BD Biosciences). The 2×10^6 cells were transferred retro-orbitally into congenic naïve CD45.1 mice. One day after transfer, the mice received OVA (grade V, Sigma) dissolved in drinking water (1.5%) for 6 days starting at ZT23 or ZT11, the transition times according to multivariate analysis (Fig. 4b). As early activation of T lymphocytes—which involves the interaction with APC—occurs already 6 h after antigen feeding[16], these ZT were selected to allow the antigen to be in MLNs at ZT5 and ZT17, respectively. The mice were euthanized on day 7 at ZT11 or ZT23, and intracellular levels of Foxp3 and T-bet were evaluated by flow cytometry in transferred OT-II+/− CD45.2+CD4+ T cells from MLNs, the lamina propria, and the spleen.

Statistical analysis

Statistical differences between groups were determined by ANOVA in one or two ways, followed by a Bonferroni post-hoc or Fischer LSD when the "*n*" per group was different. Conventional statistical analyses were performed using the GraphPadPrism 5 software (GraphPad Software, San Diego, CA). For the relative expression of clock genes and according to their gamma distribution, these data were analyzed with a generalized lineal model with Infostat software (Infostat version 2016, Universidad Nacional de Córdoba, Argentina). Significance values of $p < 0.05$ were considered statistically significant. The multivariate statistical analyses were performed with Infostat software. To perform the PCA, all the variables studied were determined in each mouse. The PCA was used as an exploratory data analysis to construct predictive models. The analysis generated new variables (principal

components) that explained data variability, and dispersion graphs (biplot) were constructed to visualize both the observations and the variables in the same space. A LDA was used to describe the relationships between two or more populations (groups), maximizing the differences. MANOVA was used to make inferences about the effects of the set of variables simultaneously.

ACKNOWLEDGEMENTS

This work was supported by Agencia Nacional de Promoción Científica y Tecnológica (FONCYT) [PICT 0117 2016 and PICT 1068 2013] and Secretaria de Ciencia y Tecnología de la Universidad Nacional de Córdoba (SECYT-UNC). We would like to thank Paula Icely, Pilar Crespo, Paula Abadie, and Fabricio Navarro for their excellent technical assistance. F.N.N. and S.G.C. belong to the CONICET research staff. B.E.B. and L.M.M. received a fellowship from CONICET.

AUTHOR CONTRIBUTIONS

B.E.B. and L.M.M. performed the experiments; B.E.B. and S.G.C. designed the study; F.N.N., B.E.B., and S.G.C. performed the statistical analysis; B.E.B. and S.G.C. wrote the paper.

ADDITIONAL INFORMATION

The online version of this article (https://doi.org/10.1038/s41385-018-0095-3) contains supplementary material, which is available to authorized users.

Competing interests: The authors declare no competing interests.

REFERENCES

1. Ripperger, J. A., Jud, C. & Albrecht, U. The daily rhythm of mice. *FEBS Lett.* **585**, 1384–1392 (2011).
2. Scheiermann, C., Gibbs, J., Ince, L. & Loudon, A. Clocking in to immunity. *Nat. Rev. Immunol.* **18**, 423–437 (2018).
3. Dunlap, J. C. Molecular bases for circadian clocks. *Cell* **96**, 271–290 (1999).
4. Voigt, R. M., Forsyth, C. B., Green, S. J., Engen, P. A. & Keshavarzian, A. Circadian rhythm and the gut microbiome. *Int. Rev. Neurobiol.* **131**, 193–205 (2016).
5. Panda, S. Circadian physiology of metabolism. *Science* **354**, 1008–1015 (2016).
6. Panda, S. & Hogenesch, J. B. It's all in the timing: many clocks, many outputs. *J. Biol. Rhythms* **19**, 374–387 (2004).
7. Cermakian, N. et al. Crosstalk between the circadian clock circuitry and the immune system. *Chronobiol. Int.* **30**, 870–878 (2013).
8. Curtis, A. M., Bellet, M. M., Sassone-Corsi, P. & O'Neill, L. A. Circadian clock proteins and immunity. *Immunity* **40**, 178–186 (2014).
9. Yu, X. et al. TH17 cell differentiation is regulated by the circadian clock. *Science* **342**, 727–730 (2013).
10. Everson, C. A. Sustained sleep deprivation impairs host defense. *Am. J. Physiol.* **265**, R1148–R1154 (1993).
11. Castanon-Cervantes, O. et al. Dysregulation of inflammatory responses by chronic circadian disruption. *J. Immunol.* **185**, 5796–5805 (2010).
12. Thaiss, C. A. et al. Microbiota diurnal rhythmicity programs host transcriptome oscillations. *Cell* **167**, 1495–1510 (2016).
13. Laermans, J. et al. Shifting the circadian rhythm of feeding in mice induces gastrointestinal, metabolic and immune alterations which are influenced by ghrelin and the core clock gene Bmal1. *PLoS ONE* **9**, e110176 (2014).
14. Novotny Nuñez, I., Barrios, B. E., Macció-Maretto, L. & Correa, S. G. Migratory capacity and function of dendritic cells from mesenteric afferent lymph nodes after feeding a single dose of vitamin A. *J. Nutr. Biochem.* **49**, 110–116 (2017).
15. Shan, M. et al. Mucus enhances gut homeostasis and oral tolerance by delivering immunoregulatory signals. *Science* **342**, 447–453 (2013).
16. Gütgemann, I., Fahrer, A. M., Altman, J. D., Davis, M. M. & Chien, Y. H. Induction of rapid T cell activation and tolerance by systemic presentation of an orally administered antigen. *Immunity* **8**, 667–673 (1998).
17. Hughes, M. E., Hogenesch, J. B. & Kornacker, K. JTK_CYCLE: an efficient nonparametric algorithm for detecting rhythmic components in genome-scale data sets. *J. Biol. Rhythms* **25**, 372–380 (2010).
18. Silver, A. C., Arjona, A., Hughes, M. E., Nitabach, M. N. & Fikrig, E. Circadian expression of clock genes in mouse macrophages, dendritic cells, and B cells. *Brain Behav. Immun.* **26**, 407–413 (2012).
19. Reppert, S. M. & Weaver, D. R. Coordination of circadian timing in mammals. *Nature* **418**, 935–941 (2002).
20. Keller, M. et al. A circadian clock in macrophages controls inflammatory immune responses. *Proc. Natl. Acad. Sci. U.S.A.* **106**, 21407–21412 (2009).
21. Froy, O. & Chapnik, N. Circadian oscillation of innate immunity components in mouse small intestine. *Mol. Immunol.* **44**, 1954–1960 (2007).
22. Druzd, D. et al. Lymphocyte circadian clocks control lymph node trafficking and adaptive immune responses. *Immunity* **46**, 120–132 (2017). 2017.
23. Silva-Sanchez, A., Randall, T. D. & Fugue, G. Minor: getting the lymph node ensemble together with circadian rhythm. *Immunity* **46**, 6–8 (2017).
24. Shiow, L. R. et al. CD69 acts downstream of interferon-alpha/beta to inhibit S1P1 and lymphocyte egress from lymphoid organs. *Nature* **440**, 540–544 (2006).
25. Tomura, M., Itoh, K. & Kanagawa, O. Naive CD4+ T lymphocytes circulate through lymphoid organs to interact with endogenous antigens and upregulate their function. *J. Immunol.* **184**, 4646–4653 (2010).
26. Cyster, J. G. & Schwab, S. R. Sphingosine-1-phosphate and lymphocyte egress from lymphoid organs. *Annu. Rev. Immunol.* **30**, 69–94 (2012).
27. Pabst, O., Bernhardt, G. & Förster, R. The impact of cell-bound antigen transport on mucosal tolerance induction. *J. Leukoc. Biol.* **82**, 795–800 (2007).
28. Barnes, M. J. & Powrie, F. Regulatory T cells reinforce intestinal homeostasis. *Immunity* **31**, 401–411 (2009).
29. Wadwa, M. et al. IL-10 downregulates CXCR3 expression on Th1 cells and interferes with their migration to intestinal inflammatory sites. *Mucosal Immunol.* **9**, 1263–1277 (2016).
30. Krause, P. et al. IL-10-producing intestinal macrophages prevent excessive antibacterial innate immunity by limiting IL-23 synthesis. *Nat. Commun.* **11**, 7055–7059 (2015).
31. Worbs, T. et al. Oral tolerance originates in the intestinal immune system and relies on antigen carriage by dendritic cells. *J. Exp. Med.* **203**, 519–527 (2006).
32. Nguyen, L. P. et al. Role and species-specific expression of colon T cell homing rceptor GPR15 in colitis. *Nat. Immunol.* **16**, 207–213 (2015).
33. Scheiermann, C. et al. Adrenergic nerves govern circadian leukocyte recruitment to tissues. *Immunity* **37**, 290–301 (2012).
34. Scheiermann, C., Kunisaki, Y. & Frenette, P. S. Circadian control of the immune system. *Nat. Rev. Immunol.* **13**, 190–198 (2013).
35. Thaiss, C. A. et al. Transkingdom control of microbiota diurnal oscillations promotes metabolic homeostasis. *Cell* **159**, 514–529 (2014).
36. Knoop, K. A. et al. Antibiotics promote the sampling of luminal antigens and bacteria via colonic goblet cell associated antigen passages. *Gut Microbes* **8**, 400–411 (2017).
37. Pagel, R. et al. Circadian rhythm disruption impairs tissue homeostasis and exacerbates chronic inflammation in the intestine. *FASEB J.* **31**, 4707–4719 (2017).
38. Diehl, G. E. et al. Microbiota restricts trafficking of bacteria to mesenteric lymph nodes by CX(3)CR1(hi) cells. *Nature* **494**, 116–120 (2013).
39. Gibbs, J. et al. An epithelial circadian clock controls pulmonary inflammation and glucocorticoid action. *Nat. Med.* **20**, 919–926 (2014).
40. Fortier, E. E. et al. Circadian variation of the response of T cells to antigen. *J. Immunol.* **187**, 6291–6300 (2011).
41. Silver, A. C., Arjona, A., Walker, W. E. & Fikrig, E. The circadian clock controls toll-like receptor 9-mediated innate and adaptive immunity. *Immunity* **36**, 251–261 (2012).
42. Tanabe, K. et al. Antigen exposure in the late light period induces severe symptoms of food allergy in an OVA-allergic mouse model. *Sci. Rep.* **5**, 14424 (2015).
43. Hadis, U. et al. Intestinal tolerance requires gut homing and expansion of FoxP3+ regulatory T cells in the lamina propria. *Immunity* **34**, 237–246 (2011).
44. Colonna, M. & Cervantes-Barragan, L. Converting to adapt. *Science* **352**, 1515–1516 (2016).
45. Sujino, T. et al. Tissue adaptation of regulatory and intraepithelial $CD4^+$ T cells controls gut inflammation. *Science* **352**, 1581–1586 (2016).
46. Sena, A. A. et al. Lack of TNFRI signaling enhances annexin A1 biological activity in intestinal inflammation. *Biochem. Pharmacol.* **98**, 422–431 (2015).
47. Mowat, A. M. & Agace, W. W. Regional specialization within the intestinal immune system. *Nat. Rev. Immunol.* **14**, 667–685 (2017).
48. Pedrotti, L. P., Sena, A. A., Rodriguez Galán, M. C., Cejas, H. & Correa, S. G. Intestinal mononuclear cells primed by systemic interleukin-12 display long-term ability to aggravate colitis in mice. *Immunology* **150**, 290–300 (2017).
49. Pedrotti, L. P. et al. Systemic IL-12 burst expands intestinal T-lymphocyte subsets bearing the $\alpha_4\beta_7$ integrin in mice. *Eur. J. Immunol.* **46**, 70–80 (2016).